Journal of Fluorescence, Vol. 13, No. 1, January 2003 (© 2003)

Intrinsic Fluorescence of Actin

Konstantin K. Turoverov[1,2] and Irina M. Kuznetsova[1]

In this work actin is used to illustrate connection of protein fluorescence characteristics with its structure. On one hand, it has been demonstrated what kind of information about the contribution of each tryptophan residues to the bulk fluorescence spectrum can be obtained from the special analysis of protein three-dimensional structure. On the other hand, potentials of intrinsic fluorescence for elucidation of proteins structure, dynamics and processes of folding-unfolding are shown. In particular, using this method a new essentially unfolded kinetic intermediate state of actin was detected and characterized, and the place of inactivated actin and its kinetic predecessor in the process of folding-unfolding was determined. It has been revealed that inactivated actin is not intermediate state between the native and completely unfolded states, as it has been accepted before, but a result of protein misfolding. On the basis of the obtained data a new model of actin folding-unfolding pathway has been proposed.

KEY WORDS: Intrinsic fluorescence of proteins; tryptophan residues; protein structure; folding-unfolding; actin.

INTRODUCTION

Tryptophan fluorescence of proteins is widely used for elucidation of their structure, folding-unfolding, and dynamics (see, e.g., [1–5]). It is due to a high sensitivity of various parameters of fluorescence of tryptophan residues (spectrum position, quantum yield, anisotropy, etc.) to properties of their microenvironment and peculiarities of their location in protein macromolecule. The dependence of intrinsic protein fluorescence on peculiarities of their tryptophan residues location was suggested from the study of intrinsic fluorescence of model compounds and proteins in different structural states. Specifically, position of the fluorescence spectrum of tryptophan residue was assumed to be mainly determined by its acceptability to solvent molecules. It is believed that intrinsic tryptophan residues unacceptable to solvent have blue fluorescent spectrum, while fluorescent spectrum of extrinsic tryptophan residues acceptable to solvent is red shifted. According to the current knowledge, the quantum yield primarily depends on the existence of quenching groups in the vicinity of tryptophan residues. It can be some groups of side chains of amino acid residues of protein or molecules of the solvent. However, the accepted concept can hardly be considered conclusively established.

Investigations of this issue have been evolving gradually. The essential progress in understanding quenching mechanisms of different functional groups of amino acid side chains, peptide bond, and solvent was obtained in the series of works of Barkley and co-workers [6–8]. Many problems such as the reason for the non-monoexponential decay law of tryptophan residues in protein and tryptophan in solution [9–12], participation of oscillators ^1L_a и ^1L_b in emission [13], factors determining fluorescence spectrum position in proteins [14], etc., are still actual. In the works of Burstein and co-workers [15–17], the idea of statistically discrete classes of the residues emitting in protein, which reflects the difference of the connection of excited states of tryptophans with their environments is substantiated.

From our viewpoint, the properties of the tryptophan residues location and, hence, of their fluorescent charac-

[1] Institute of Cytology of the Russian Academy of Science, St. Petersburg, 196064, Russia.
[2] To whom correspondence should be addressed. E. mail: kkt@mail.cytspb.rssi.ru

1053-0509/03/0100–0041/0 © 2003 Plenum Publishing Corporation

teristics are especially individual. The idea of analyzing simultaneously the characteristics of proteins intrinsic fluorescence and their three-dimensional (3D) structure to establish the dependence of fluorescence characteristics on peculiarities of the tryptophan residues location in protein structure [18] has been arisen in connection with the determination of 3D structures of many proteins by x-ray analysis up to the co-ordinates of individual atoms and its availability from the Protein Data Bank [19]. Such analysis facilitates the interpretation of proteins fluorescence characteristics and allows improving knowledge of the dependence of recorded fluorescent characteristics of tryptophan residues on the peculiarities of its microenvironment [20–24]. Carrying out of such studies on recombinant proteins with changed tryptophan residues or some other residues in its vicinity increases essentially the experimental basis of such works (see, e.g., [25–28]).

The goal of our work was, on one hand, to show, using actin from rabbit skeletal muscle as an example, how the recorded fluorescent characteristics depend on properties of microenvironment and peculiarities of location of its tryptophan residues and, on the other hand, to demonstrate opportunities of this method for studying the protein folding-unfolding process and properties of the folding intermediate as well as misfolded states and their aggregated forms.

INTRINSIC FLUORESCENCE OF NATIVE ACTIN AND MICROENVIRONMENT OF ITS TRYPTOPHAN RESIDUES

Actin is one of the major proteins of muscle tissues and cytoskeleton of non-muscle eukaryotic cells [29,30]. At low ionic strength actin exists as a monomer (G-actin), whereas in the presence of neutral salts it is polymerized into a double-stranded polymer (the so-called fibrous form of actin, or F-actin). F-actin forms the backbone of thin filaments in muscle fibers. The 3D structure of actin was determined for complexes of actin with proteins that prevent its polymerization, namely DNase I [31], gelsoline [32,33], and profiline [34], as well as for ADP-actin modified by tetramethyl-rhodamine-5-maleimide [35]. G-actin globule (42 kDa) is formed by the single polypeptide chain containing 375 amino acids. It consists of two major domains, each divided into two subdomains. Actin is known to bind one molecule of ATP (or ADP) and one divalent Mg^{2+} cation. When investigated in vitro, Mg^{2+} is usually substituted by Ca^{2+}. Both nucleotide and divalent cation are located in the slit between two domains (Fig. 1).

The position and the form of protein fluorescence spectrum are determined by superposition of fluorescence spectra of its individual tryptophan residues by their

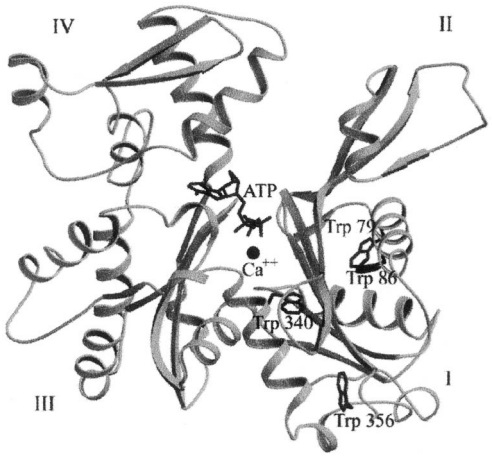

Fig. 1. The structure of actin macromolecule. Subdomains are indicated by roman numbers according to Ref. 31. Tryptophan residues Trp79, Trp86, Trp340, and Trp356, ATP, and Ca^{++} are shown.

position in the wavelength scale and their relative contribution to the integrated protein radiation. Actin contains four tryptophan residues. The fluorescence spectrum of native actin is a relatively blue one (λ_{max} = 325 nm [36,37]; Fig. 2). The value of parameter $A = I_{320}/I_{365}$, representing the ratio of fluorescence intensities at 320 and 365 nm, amounts for native actin to 2.6 [36]. Only some tryptophan containing proteins (e.g., azurin *Pseudonomas aeruginosa* [38], RNase T1 [39], RNase C2 [21], and parvalbumin merlange [40]) have more blue fluorescence spectrum. The blue fluorescence spectrum

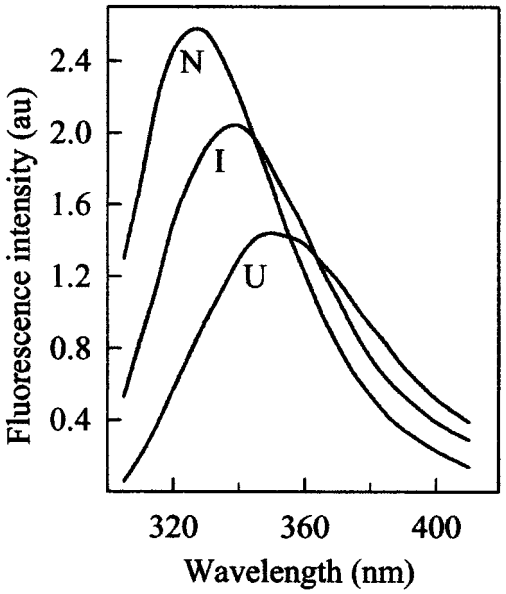

Fig. 2. Fluorescence spectra of native (N), inactivated (I), and completely unfolded (6 M GdmCl; U) actin. λ_{ex} = 297 nm.

of actin might have been explained based on the analysis of microenvironments of each tryptophan residue. This analysis was done on the bases of atoms coordinates of actin DNase I complex 3D structure (file Pdb1atn.ent in the Protein Data Bank [19,31]). It was taken that the structure of free actin and actin in complex with DNase I is the same. All four tryptophan residues of actin are located in subdomain I [31]. Tryptophan residues Trp79, Trp86, and Trp340 are incorporated in α-helix formed by Trp79-Asn92 and Ser338-Ser348. Tryptophan residue Trp356 is situated in the unstructured region between α-helixes Ser350-Met355 and Lys359-Ala365 (Fig. 3).

Position of Individual Tryptophan Fluorescence Spectrum

The position in the wavelength scale depends on the polarity of its microenvironment and its ability to relax during the tryptophan residue fluorescence lifetime (i.e., subnanosecond and nanosecond time scale). The blue spectrum in principle can appear in two cases—if the tryptophan residue is located in the hydrophobic microenvironment independently on microenvironment relaxation properties or if the microenvironment is rigid even if it is polar. In the latter case the radiation appears from the unrelaxed state. The polarity of the tryptophan residue microenvironment is determined by the accessibility of tryptophan residues to the solvent molecules and by the existence of polar groups of amino acid side chains of protein in its vicinity.

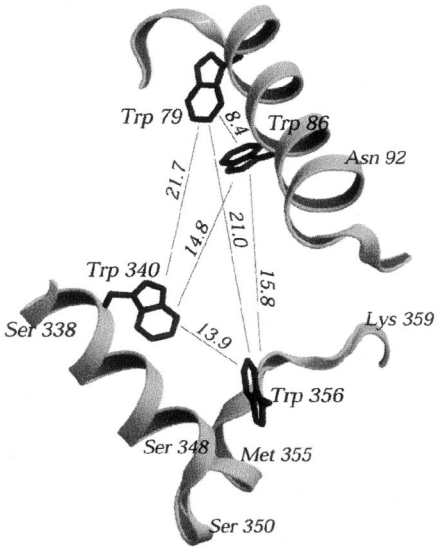

Fig. 3. Location of tryptophan residues in actin macromolecule. The distances between the geometrical centers of indole rings of tryptophan residues are given in Å.

The special analysis of the peculiarities of tryptophan residue location in protein which can affect its fluorescence characteristics [18,23,41] was used. This analysis includes determination of conformation of tryptophan residues side chain, identification of its nearest neighborhoods along the polypeptide chain and conformation of the part of polypeptide chain where it is located. A special attention is paid to the analysis of tryptophan residue microenvironment. Microenvironment of tryptophan residue is determined as a set of atoms which are no greater than r_0 distant from the geometrical center of the indole ring. To take into account all atoms that can contact the indole ring, the value of r_0 was chosen as 7 Å [18,41]. For all atoms of microenvironment the distance from the geometrical center of the indole ring and their location relative to the indole ring are determined (Table I).

One of the characteristics of microenvironment is packing density of atoms, which is determined as a number of atoms which compose microenvironment, or the part of microenvironment volume (V_0) occupied by atoms

$$d = \frac{\Sigma V_i}{V_0} \tag{1}$$

The volume of each atom (V_i) is determined on the basis of its Van der Waals radius and only the part of the volume which is inside microenvironment is taken into account. This estimation is of course not exact because in reality atoms are incorporated by chemical bonds and occupy a smaller volume. Nonetheless it is not significant for comparative estimation of packing density of microenvironment of different tryptophan residues.

It is generally accepted that fluorescent characteristics of tryptophan residues to a great extend depend on their accessibility to the solvent. The exposure of tryptophan residues to the solvent molecules depends not only on the packing density of its microenvironment, but also on its location in the protein macromolecule, i.e., whether it is located near the center of protein macromolecule or at the periphery. To estimate the accessibility of tryptophan residues to the solvent, the radial dependence of atoms packing density about the geometrical center of tryptophan residue was evaluated as

$$d(r) = \frac{\Sigma V_i(r,\, r + \Delta r)}{V_0(r,\, r + \Delta r)} \tag{2}$$

where V_0 $(r, r + \Delta r)$ is the volume of sphere layer, that is r distant from the geometrical center of the indole ring, Δr is layer thickness and V_i is the part of the i's atom volume that is inside this sphere layer.

The analysis of the 3D structure of the actin macromolecule shows that packing density of individual tryp-

Table I. Amino Acid Side Chains: Potential Quenchers of Tryptophan Fluorescence in Actin

			Distance between O, N, and S Atoms of Microenvironments and All Atoms of Tryptophan Residues (in Å)													
Trp	Residue	Atom	N	CA	C	O	CB	CG	CD1	CD2	NE1	CE2	CE3	CZ2	CZ3	CH2	Centre
79	Asn115	OD1	9.26	9.39	10.84	11.25	8.67	7.13	6.52	6.41	5.23	5.10	6.88	**4.12**	6.18	4.82	5.62
	Asn115	ND2	8.69	8.86	10.32	10.68	8.48	6.99	6.59	6.13	5.32	4.93	6.40	**3.81**	5.56	4.24	5.35
	Lys118	NZ	6.87	5.90	6.20	6.11	4.43	**4.55**	5.13	4.82	5.66	5.51	5.05	6.33	5.91	6.49	5.23
	Met119	SD	10.70	10.00	10.90	10.51	9.68	8.71	9.35	7.34	8.53	7.25	6.31	6.17	4.99	**4.91**	6.99
86	Cys10	SG	6.79	6.10	7.01	6.72	6.28	5.41	4.09	6.10	**4.04**	5.30	7.43	6.09	7.99	7.43	5.86
	Asn12	OD1	6.17	6.13	7.51	7.78	6.14	4.85	3.72	4.98	**2.92**	3.82	6.14	4.16	6.33	5.50	4.49
	Asn12	ND2	8.06	7.86	9.24	9.48	7.54	6.10	5.12	5.86	**3.99**	4.49	6.80	4.21	6.60	5.43	5.18
	Met82	SD	6.06	6.93	8.34	9.22	6.83	5.89	5.83	5.42	5.27	4.98	5.72	**4.85**	5.59	5.17	5.12
	Met119	SD	11.43	11.19	12.48	13.05	10.12	8.77	8.71	7.65	7.52	6.75	7.48	5.43	6.29	**5.15**	6.96
	Met123	SD	8.11	7.00	7.45	7.62	5.71	5.32	5.75	5.05	5.74	5.33	**5.08**	5.63	5.38	5.65	5.14
340	Asp24	OD2	11.86	10.50	9.88	9.32	9.81	8.51	8.67	7.25	7.57	6.57	6.80	5.25	5.51	**4.59**	6.64
	Ser344	OG	8.32	7.14	5.88	4.97	7.40	6.66	7.31	5.54	6.73	5.63	4.77	4.95	**3.95**	4.06	5.33
356	Asp3	OD1	9.49	9.25	10.23	10.27	7.89	6.97	5.98	7.26	**5.56**	6.36	8.33	6.69	8.56	7.82	6.89
	Asp3	OD2	8.78	8.31	9.03	8.89	6.85	6.22	5.52	6.60	**5.42**	6.08	7.57	6.64	8.00	7.59	6.43

The distances between atoms of microenvironment and the nearest atom of the indole ring are shown in bold.

tophan residues microenvironments varies greatly (Table II). Thus, in the sphere of 7 Å in radius, which center coincides with geometrical center of the indole ring of analyzed tryptophan residue, there are 50, 61, 78, and 69 atoms of the protein for tryptophan residues Trp79, Trp86, Trp340, and Trp356, respectively. For comparison, there are 71 atoms in the microenvironment of the inner tryptophan residue of azurin [18], which has the most unique blue fluorescence spectrum (λ_{max} = 308 nm [38]). Thus, two tryptophan residues of actin—Trp340 and Trp356—have a very high density of microenvironment (d = 0.84 and 0.76). Although they are located not in the center protein macromolecule but closer to its periphery (the value of d decreases rapidly with increase of r; Fig. 4), they are apparently inaccessible to the solvent.

Table II. Characteristics of Microenvironments and Conformation of the Side Chains of Tryptophan Residues of Actin

Conformation of the Side Chain of Tryptophan Residues and Packing Density of Their Microenvironments					Aromatic Rings and Proline Residues Involved in the Micro-environment of Tryptophan Residue		Peptide Bonds in the Microenvironment of Tryptophan Residue	
Residue	N	d	χ_2 (°)	χ_2 (°)	Residue	R (Å)	n	No. of Residues Forming Peptide Bonds
Trp79	50	0.60	295	95	Trp86	6.4–10.6	4	Ile76-Thr77; Thr77-Asn78; Asn78-Trp79; Trp79-Asp80
Trp86	61	0.70	282	325	Trp79	6.7–8.9	4	Met82-Gly83; Gly83-Lys84; Ile85-Trp86; Trp86-His87
					Phe90	6.2–8.0		
					Phe127	5.1–7.5		
Trp340	78	0.84	190	89	Phe21	8.5–9.4	11	Val9-Cys10; Lys18-Ala19; Ala19-Gly20; Gly20-Phe21;
					Pro27	3.9–4.8		Phe21-Ala22; Asp25-Ala26; Ala26-Pro27; Pro27-Arg28;
					Tyr337	6.8–9.4		Val339-Trp340; Trp340-Ile341; Ile341-Gly342
Trp356	69	0.76	282	115	Pro102	4.1–6.2	6	Pro102-Thr103; Thr103-Leu104; Ala131-Met132;
					Pro130	8.0–9.2		Met132-Tyr133; Met355-Trp356; Trp356-Ile357
					Tyr133	5.8–9.0		
					Phe352	3.5–6.0		

N is the number of atoms in the microenvironment of tryptophan residue; d is the density of tryptophan residue microenvironment; χ_1 and χ_2 are the angle, that characterize the conformation of tryptophan residue side chain; R is the distance of the aromatic rings and proline residues involved in the microenvironment of tryptophan residue from the geometrical center of its indole ring (minimal and maximal values are given); n is the number of peptide bonds in the microenvironment of tryptophan residue.

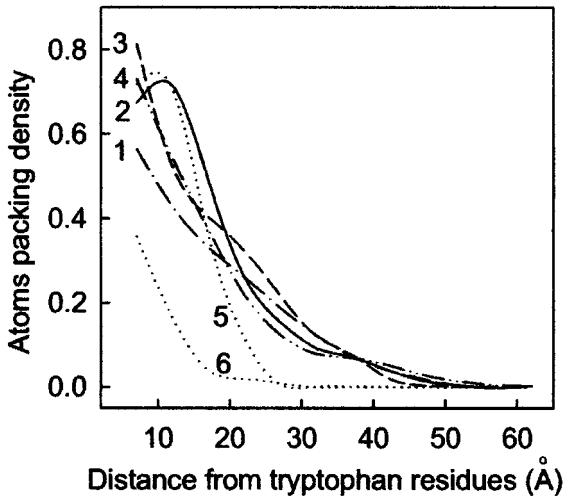

Fig. 4. Radial dependence of packing density of atoms in macromolecule about geometrical centers of indole rings of tryptophan residues in actin. Curves 1–4 are the dependences for Trp79, Trp86, Trp340, and Trp356 consequently. For comparison the dependence for Trp48 of azurin (internal tryptophan residues) and Trp19 of melittin (external tryptophan residues) are given (curves 5 and 6).

The distinctive feature of microenvironments of tryptophan residues Trp340 and Trp356 is the existence of aromatic rings of tyrosine and phenylalanine residue and rings of proline (Table II). So there are phenol ring of Tyr337 and the ring of Pro27 in the close vicinity of tryptophan residue Trp340, and aromatic ring of Phe352 and Tyr133 and the ring of Pro102 in vicinity tryptophan residue Trp356. Similar clusters of aromatic residues were found in the proteins with one tryptophan residue, which have blue fluorescent spectrum such as azurin, ribonuclease T1, and L-asparaginase [41]. The very high packing density of microenvironment of Trp340 can be explained by the location of proline residue Pro27, which has immediate contact with it. Interesting, the interconnection of tryptophan residues and proline can initiate the folding of even small polypeptide chains [42,43].

It is noteworthy that tryptophan residue Trp340 is t-conformer ($\chi_1 = 190^0$, $\chi_2 = 89^0$) unlike other tryptophan residues of actin and tryptophan residues of many other proteins [41]. The same conformation of the side chain was found for inner tryptophan residues with extremely blue fluorescence spectrum, like Trp48 of azurin and Trp59 of ribonuclease T1, and for tryptophan residue completely exposed to the solvent, like Trp25 of glucagon and Trp19 of melittin [41]. Thus, it can be the unstrained side chain conformation. At the same time the microenvironment of tryptophan residue Trp340 is very closely packed. Its packing density is even higher than that of microenvironments of tryptophan residue Trp48 of azurin ($d = 0.75$) and Trp59 of ribonuclease T1 ($d = 0.80$). Furthermore the oscillations of tryptophan residue Trp340 are restricted by proline residue Pro27, the ring of which is practically parallel to the indole ring. It is not improbable that unstrained conformation of the side chain of tryptophan residue Trp340, as well as the existence of aromatic rings of tyrosine and phenylalanine residues and proline residue, is essential for the formation of blue fluorescence spectrum of actin.

The packing density of microenvironment of Trp86 is lower than that of Trp340 and Trp356 (Table II). At the same time Figure 4 shows that this tryptophan residue is located far from proteins periphery, and it evidently also is inaccessible to the solvent. Hence, the only tryptophan residue that can be regarded as exposed to the solvent is Trp79.

The averaged experimental characteristic of tryptophan residue exposure can be obtained from fluorescence quenching by the external quencher [44]. The experiments on tryptophan fluorescence quenching of actin revealed the low accessibility of tryptophan residues to the molecules of polar quencher acrylamide [45]. The low value of quenching constant indicates that tryptophan residues are inaccessible to the solvent. It correlates with the very blue fluorescence spectrum of this protein. The blue emission spectrum of actin fluorescence and the low efficiency of fluorescence quenching by acrylamide can be explained if the contribution of tryptophan residues Trp79 (that is exposed to the solvent) to protein intrinsic fluorescence is low.

Contribution of Individual Residue to the Total Fluorescence of Protein

The quantum yield of tryptophan fluorescence primarily depends on the existence of quenching groups in its microenvironment and on the long-range effects such as Trp-Trp nonradiative energy transfer and excited-state electron transfer from the indole ring to an electron acceptor. The conformation of tryptophan residues side chain, polarity of its microenvironment and exposure to the solvent also can affect the value of the quantum yield.

Analysis of the actin structure reveals that microenvironments of both Trp79 and Trp86 tryptophan residues contain sulfur atoms of methionine and cysteine residues (Table I), which are known to be effective fluorescence quenchers [46]. These are sulfur atoms of Met119 in the vicinity of Trp79 and sulfur atoms of Met82, Met119, Met123, and Cys10 in the environment of Trp86. Furthermore, the amide group of Asn115 and amino group of Lys118 can be potential quenching groups for tryptophan

residue Trp79, while the amide group of Asn12 can be a potential quenching group for tryptophan residue Trp86.

Analysis of the dependence of fluorescent quantum yield on the peculiar features of microenvironments of tryptophan residues for a number of proteins revealed that the efficiency of quenching depends not only on the proximity of quenching group to the indole ring but, to a great extent, also on the location of this group relative to the indole rings of tryptophan residues [41]. A number of sulfur atoms in the vicinity of the indole ring of tryptophan residue Trp86 and especially the immediate neighborhood of SG of Cys10 to NE1 of the indole ring of Trp86 (Table I) allows considering this tryptophan residue as practically completely quenched.

Additional information on the contribution of individual tryptophan residues to the bulk fluorescence of actin can be obtained by evaluating the efficiency of nonradiative energy transfer between these tryptophan residue. The distances between the geometrical centers of the indole rings of tryptophan residues and their mutual orientation (Fig. 3.) were determined based on the 3D structure of actin. The efficiency of nonradiative energy transfer between tryptophan residues was evaluated as follows [47]

$$W = \frac{1}{1 + \frac{2/3}{k^2}\left(\frac{R}{R_0}\right)^6} \qquad (3)$$

where R_0 is the so-called critical Forster distance, R is the distance between the geometrical centers of the indole rings of donor and acceptor, and k^2 is the factor of mutual orientation of donor and acceptor.

$$k^2 = (\cos\theta - 3\cos\theta_A\cos\theta_D)^2 \qquad (4)$$

where θ is the angle between the directions of the emission oscillator of donor and absorption oscillator of acceptor; θ_A and θ_D are the angles between these oscillators and the vector connecting the geometrical centers of donor and acceptor [48]. In these evaluations R_0 is taken from literature, while other values are determined on the basis of atoms co-ordinates [18,41]. The calculations were done assuming model of rigid oscillators. In consequence of uncertainty of donor quantum yield and overlap integral donor fluorescence and acceptor absorption the value of W for Trp-Trp energy transfer was calculated with two values of R_0 - 7.8 and 8.7 Å [49,50]. The effective nonradiative energy transfer between tryptophan residues Trp79 and Trp86 was revealed (Table III). Consequently, even if tryptophan residue Trp79 is not quenched by SD atom of Met119, it nonetheless must have low quantum yield due to effective energy transfer to Trp86. The calculations show that nonradiative energy transfer between other tryptophan residues is of low efficiency (Table III).

Table III. Nonradiative Energy Transfer between Tryptophan Residues in Actin*

Residue	Trp79	Trp86	Trp340	Trp356
Trp79	—	0.64–0.77	0.01–0.02	0.01–0.02
Trp86	1.6	—	0.11–0.19	0.00–0.01
Trp340	2.7	3.4	—	0.05–0.09
Trp356	2.8	0.1	1.0	—

Table shows the values of the efficiency of nonradiative energy transfer W calculated with two values of R_0: 7.8 and 8.7 Å [40,41] (upper right) and orientation factors k^2 (lower left). These values were calculated according to Eqs. (3) and (4). The distances between the geometrical centers of the indole rings of tryptophan residues, needed for the evaluation of nonradiative energy transfer, are given in Figure 3.

Carboxyl groups of aspartic and glutamic acids are most likely to be effective quenchers of tryptophan fluorescence in protonated form and do not quench at neutral pH. Nothing is known about quenching action of hydroxyl groups of serine and threonine. That is why, though atoms OD2 of Asp24, OG Ser344, and OD1 and OD2 of Asp3 are incorporated in the microenvironment of tryptophan residues Trp340 and Trp356 (Table I), it is unlikely that they could affect fluorescent characteristics of these tryptophan residues.

Hence, the intrinsic UV-fluorescence of the native actin is mainly determined by tryptophan residues Trp340 and Trp356, which are practically inaccessible to the solute molecules. The microenvironments of these residues are formed mainly by nonpolar groups of protein and closely packed (Tables I and II). At the same time tryptophan residues Trp79 and Trp86, located in polar environment, are quenched and give minimal contribution to the bulk fluorescence of actin. All our conclusions concerning the contributions of individual tryptophan residues to the bulk actin fluorescence [23] were completely confirmed by Doyle et al. [28]. In this work the fluorescent properties of mutant forms of yeast actin with tryptophan changed to other amino acids were studied.

The above analysis of the tryptophan residues' microenvironments ignored the presence of the large number of peptide bonds in the microenvironment of tryptophan residue (Table II). Interestingly, the greatest number of peptide bonds were found in the environment of tryptophan residues Trp340 and Trp356, which give the greatest contribution to the bulk actin fluorescence. Hence, although the quenching effect of peptide groups on the fluorescence of model componeds containing the indole ring in solution has been shown [6,7], the questing about the effect of the peptide bonds on the value of

quantum yield and fluorescence spectrum position of tryptophan residues in proteins still remains open.

INACTIVATED ACTIN AND ITS FLUORESCENCE CHARACTERISTICS

The release of calcium ion by EDTA or EGTA treatment leads to transformation of G-actin into the inactivated form, in which the protein molecule loses its capability to polymerize [45,51]. Inactivated actin also may be obtained as a result of heat denaturation [45,51–62], a moderate urea or guanidinium chloride (GdmCl) concentration [45,59], dialysis from 8 M urea or 6 M GdmCl [59,60], or spontaneously during storage [59]. The fluorescence spectrum of inactivated actin, being considerably different from that of native protein (λ_{max} = 340 nm, A = 1.3), still remains a substantial blue shift as compared with the spectrum of completely unfolded protein (λ_{max} = 350 nm, A = 0.4; see also Fig. 2). Properties of inactivated actin are invariant to the way of denaturation [45,59,63,64] Until recently, inactivated actin has been believed to be intermediate state between native actin and completely unfolded protein. The new view on the place of inactivated actin in the process of protein folding-unfolding will be discussed below.

Exposure of Tryptophan Residues to the Solvent

As mentioned above, protein fluorescence spectrum is determined by polarity of tryptophan residues microenvironment—the accessibility of tryptophan residues to the solvent and the presence of polar groups of protein amino acids in their close vicinity. When analyzing results of fluorescence measurements of proteins this notion is often used in a simplified manner. Usually it is accepted that the position of fluorescence spectrum of tryptophan residues is dictated by their accessibility to solvent molecules only. The red shifted fluorescence spectrum of inactivated actin had also been explained by partial exposure of tryptophan residues to the aqueous environment [37,60]. Really, tryptophan residue Trp25 of glucagon is exposed to the solvent and this protein have red shifted fluorescence spectrum, while tryptophan residue Trp48 of azurine is located in the inner part of macromolecule and this protein have the unique blue fluorescence spectra. At the same, time inaccessibility to the solvent is not the only condition of the appearance of blue fluorescence spectrum. It is to be taken into account that polarity of microenvironment of tryptophan residues is determined not only by its exposure to the solvent but also by intrinsic polar groups of amino acid side chains included in the microenvironment of this tryptophan residue.

To verify whether the tryptophan residue is exposed to the solvent, or is localized in interior inaccessible to solvent parts of protein macromolecules, quenching of tryptophan fluorescence by acrylamide can be analyzed. For constructing the Stern-Volmer plots a diminishing of the fluorescence intensity (I) or a change of mean fluorescence life-time ($\bar{\tau}$) with increase of acrylamide concentration [Q] can be recorded. The Stern-Volmer plots for steady-state measurements, i.e., experimental plots I/I_0 vs [Q], were found to be upward curving for both native and inactivated actin. It means that along with dynamic there is also static quenching. In this case Stern-Volmer plot is as follows [44]

$$I_0/I = 1 + \langle K \rangle [Q] \exp(V[Q]) \quad (5)$$

Here I and I_0 are intensities of fluorescence in the absence and in the presence of quencher at molar concentration [Q], and V and $\langle K \rangle$ are static and dynamic quenching constants. In such case, for evaluation Stern-Volmer constant $\langle K \rangle$ Stern-Volmer plots for time-resolved measurements must be constructed [44]

$$\bar{\tau}/\bar{\tau}_0 = 1 + \langle K \rangle [Q] \quad (6)$$

Here $\bar{\tau}$ and $\bar{\tau}_0$ are weighted mean life times ($\bar{\tau} = \Sigma \alpha_i \tau_i$) determined in the absence and in the presence of quencher at molar concentration [Q], $\langle K \rangle$ is the dynamic quenching constant. The dynamic constant is equal to $k_q \langle \tau_0 \rangle$, where k_q is bimolecular rate constant for the quenching process and $\langle \tau_0 \rangle$ is the root-mean square value of fluorescence lifetime in the absence of quencher [44].

The mean life times were determined on the base of fluorescence decay curves. The fluorescence decay curves were recorded both for native and inactivated actin in the absence of acrylamide (Fig. 5) and in the presence of appropriate concentration of quencher. The fluorescence decay curves of both native and inactivated actin cannot be satisfactory fitted by monoexponential function but can be accurately described by biexponential law. As the multiexponential decay was described even for proteins with one tryptophan residue, or for model compounds in solution [65], the biexponential decay of actin cannot be explained only by the existence of several tryptophan residues. The measured lifetimes of the tryptophan fluorescence were used and bimolecular quenching constant by extrinsic polar quencher acrylamide and for the analysis of fluorescence anisotropy data and evaluation of intramolecular mobility (see below). It is to be mentioned that for construction Stren-Volmer plot the weighted mean life-time $\bar{\tau}$ must be used, while for evaluation bimolecular rate constant of quenching process and

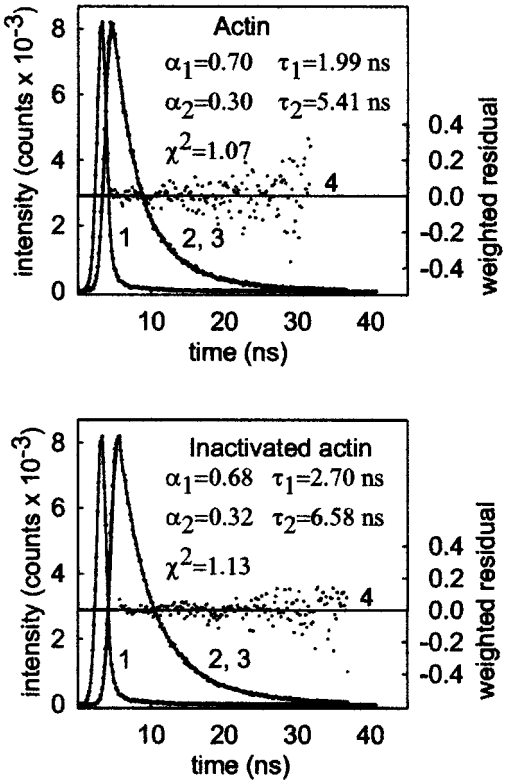

Fig. 5. Decay curve of tryptophan residues fluorescence in native and inactivated actin. Figure represents excitation lamp profile (curve 1), experimental decay curve (curve 2), best fitted calculated fluorescence decay curve (curve 3), and deviation between the experimental and calculated decay curve (weighted residuals; curve 4). The excitation wavelength was 297 nm, and the registration wavelength was 350 nm.

for evaluating intramolecular mobility the root-mean-square value of fluorescence life-time $\langle\tau\rangle$ must be used. For biexponential decay:

$$\langle\tau\rangle = \frac{\alpha_1\tau_1^2 + \alpha_2\tau_2^2}{\alpha_1\tau_1 + \alpha_2\tau_2} = \Sigma f_i\tau_i \qquad (7)$$

It appeared that the slope of the Stern-Volmer plot and the corresponding Stern-Volmer constant $\langle K\rangle$ as well as the bimolecular rate constant of collision process (k_q) for native and inactivated actin are rather low in comparison with other proteins (Fig. 6, Table IV). These values increase considerably only in the completely unfolded protein. Interestingly, the Stern-Volmer plot and the corresponding constants for inactivated actin appeared even smaller than that for native actin. This mean that both in native and inactivated actin tryptophan residues are located in the inner parts of protein macromolecule and that tryptophan residues of inactivated actin appear to be even less accessible to solvent molecules than those of native protein.

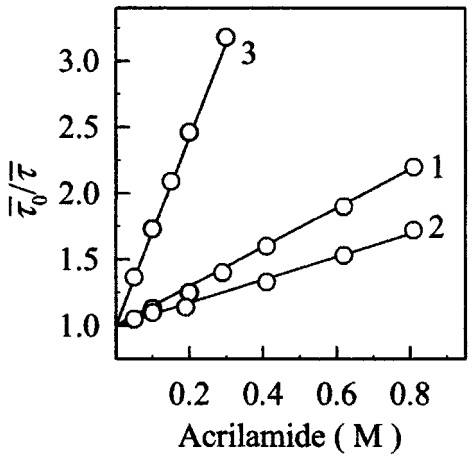

Fig. 6. Stern-Volmer plots for different actin conformations: native G-actin (curve 1), inactivated actin in 0.8 M GdmCl (curve 2), and completely unfolded protein in 5.0 M GdmCl (curve 3). The figure represent the results of intrinsic fluorescence quenching by acrylamide, monitored by tryptophan residues lifetime changes. λ_{ex} = 297 nm

Intramolecular Mobility of Tryptophan Residues

While evaluating relaxation properties of protein structure, it is necessary to distinguish between the mobility of microenvironment of tryptophan residues and the mobility of indole rings themselves. The information about the mobility of the tryptophan residue microenvironment could be obtained from the position of fluorescence spectrum and from the intensity of CD spectrum in near UV region, while the information about the mobility of tryptophan residues gives the value of their fluorescence anisotropy. Earlier we have shown that a pronounced red shift of tryptophan fluorescence does not necessarily reflect the considerable increase in its environment mobility [66,67]. And inactivated actin is a dramatic example of the situation when red shift of fluorescence spectra is accompanied by immobilization of its tryptophan resides by polar groups side chains of amino acids.

Actin inactivation is accompanied by a significant increase of fluorescence anisotropy (Fig. 7). The increase of fluorescence anisotropy can be dictated both by decrease of tryptophan residue mobility or by association of partially-folded proteins. The latter reason seems certainly true as inactivated actin has been shown to be a thermodynamically stable monodisperse associate, consisting of 15 monomers [68].

For estimation the mobility of the tryptophan residues the Perrin plots ($1/r$ versus T/η dependence) were constructed for the native, inactivated, and completely unfolded actin molecules (Fig. 8). It can be seen that actin inactivation is characterized by independence of $1/r$ on T/η (Fig. 8; curve 2). This reflects the association

Table IV. Kinetic Characteristics of Tryptophan Fluorescence of Actin and Its Quenching Constants by Acrylamide

Actin	τ_1 (ns)	α_1	τ_2 (ns)	α_2	$\langle\tau\rangle$ (ns)	k_q ($\times 10^9$ M^{-1} s^{-1})	K (M^{-1})	V (M^{-1})
Native	1.99	0.70	5.41	0.30	3.83	0.43	1.65	0.68
Inactivated	2.70	0.68	6.58	0.32	4.77	0.16	0.76	1.18

of partially-folded actin molecules in particles whose rotational relaxation time is much greater than the fluorescence lifetime. The same independence of $1/r$ on T/η takes place for F-actin which is known to be long rigid filaments comprised of numerous actin molecules (Fig. 8; curve 4).

Analysis of Figure 8 shows that the value of the intercept cut by the Perrin plot on the y axis ($1/r_0'$) both for the native and inactivated actin exceeds that for low-molecular-weight model compounds, such as *N*-acetyltryptophan, etc. ($1/r_0$). This means that in these two conformations the tryptophan residues participate in the high-frequency intramolecular mobility whose rotational relaxation time is much shorter than the excited state lifetime [66,67]. Alternatively, these tryptophan residues can be involved in the intramolecular mobility of the nanosecond time scale whose rotational relaxation time does not depend on the solvent viscosity [66,67]. The existence of the latter type of intramolecular mobility seems to be possible, since tryptophan residues of native and inactivated actin are inaccessible to solvent molecules (see the above experiments with acrylamide quenching). The fact that $(1/r_0')_{\text{G-actin}} = (1/r_0')_{\text{F-actin}}$ and $(1/r_0')_{\text{I-actin}} < (1/r_0')_{\text{G-actin}}$ indicates that the amplitude of high-frequency intramolecular mobility or rotational relaxation time invariant of solvent viscosity of native actin in G- and polymerized F-form is the same, while in the inactivated actin, the mobility of tryptophan residues is much lower.

Hence we can conclude that though the fluorescence spectrum of inactivated actin is red shifted in comparison with native actin its tryptophan residues are not exposed to the solvent, and that their microenvironment is formed by polar groups of amino acids of protein which significantly immobilize their intramolecular mobility. It has also been shown that inactivated actin has a unique structure: hydrophobic clusters are on the surface of associate, while the polar regions, in which tryptophan residues are founded to be included, are in the interior, inaccessible to solvent regions of associate [45,63,68].

ACTIN FOLDING-UNFOLDING

Study of processes of proteins folding-unfolding, detection and examination of properties of intermediate and misfolded states, which appear in these processes, is one of the main approaches to evaluate pathways of the polypeptide chain folding in a unique structure, which

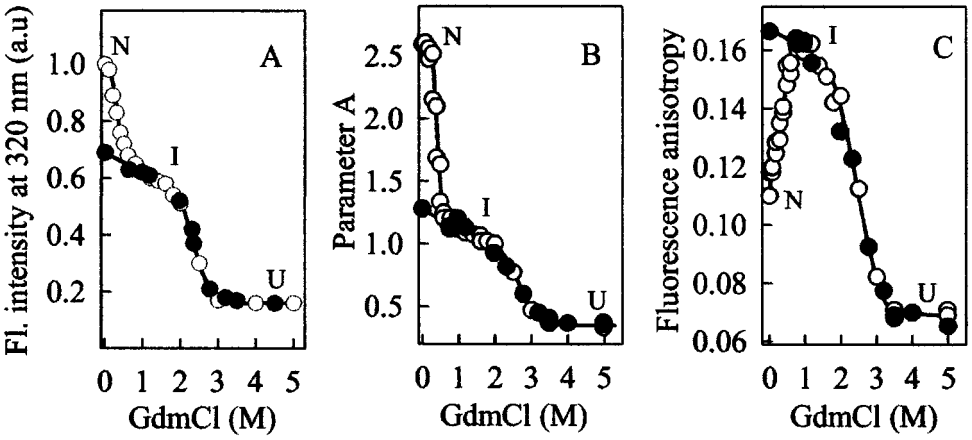

Fig. 7. GdmCl-induced structural changes of actin. Figure shows the changes of the value of parameter $A = (I_{320}/I_{365})_{297}$, that characterize of fluorescence spectrum position (A), degree of fluorescence anisotropy (B), and fluorescence intensity at 320 nm (C). The fluorescence characteristics of actin were recorded after 24 h of incubation in the definite concentrations of GdmCl. Open and filled symbols correspond to the unfolding and refolding experiments. The excitation wavelength was 297 nm. Fluorescence anisotropy was recorded at 365 nm.

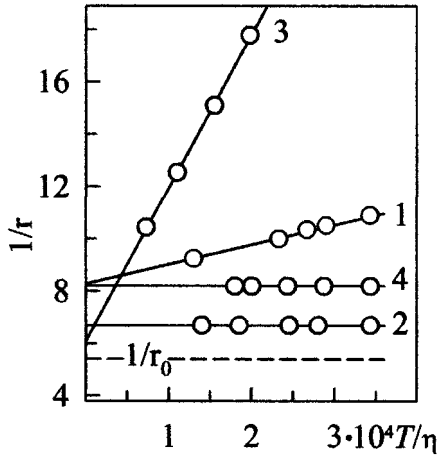

Fig. 8. Fluorescence spectra and Perrin plots of native actin (curve 1), inactivated actin (curve 2), actin in 8M urea (curve 3) and F-actin (curve 4). The excitation wavelength was 297 nm. The wavelength of recording fluorescence anisotropy was 365 nm. Solvent viscosity was varied by changing water: glycerol ratio. Temperature was 25° C.

provides a possibility of protein function. The misfolded states appeared in the process of protein folding-infolding are often stabilized by association and aggregation. As this takes place, both amorphous and ordered aggregates amiloid fibrils could appear [69–77]. The appearance of amorphous aggregates and their accumulation in the inclusion bodies in the processes of recombinant proteins superexpression is a great problem of biotechnology [78–84]. The ordered association of proteins with formation of insoluble amiloid fibrils and their deposition in different organs results in development of such severe pathologies as Alzheimer's and Parkinson's diseases, malignant myeloma, cataracts, prion afflictions, and other abnormalities [76,85–94]. Therefore, studies of partially folded and misfolded states are of crucial importance not only for solving fundamental problem of protein folding but also for medicine and biotechnology. The fluorescent approaches and intrinsic proteins fluorescence in particular are currently of intensive use in analysis of processes of protein folding-unfolding and of properties of intermediate partially-folded and misfolded states, as well as their aggregated forms.

In all studies dealing with to actin unfolding it has been assumed that actin successively transfers from the native to inactivated and then to the completely unfolded state [37,45,51–59]:

$$N \rightarrow I \rightleftarrows U \qquad (8)$$

That is, the inactivated actin (I) was considered as on-pathway intermediate between the native (N) and the completely unfolded (U) states. All equilibrium experiments appeared to support this model. In fact, data presented in Figure 7 suggest that GdmCl induces two successive conformational transitions in actin. The transition from the native to the inactivated actin takes place at low GdmCl concentrations (0.0–0.8 M), whereas transformation of the inactivated actin into the completely unfolded protein occurs between 1.8 and 4.0 M GdmCl. It also suggests that in relatively wide range of GdmCl concentrations, between 0.8 and 1.8 M, actin exists in its inactivated form. It is to be emphasized that the transition from the native to the inactivated state is irreversible [45,60–63]. Thus, all structural characteristics of actin in the range of low denaturant concentration (from 0 to 0.8 M GdmCl) are quasi-stationary. In this regard it should be noted that the curves in Figure 7 were recorded after 24-h incubation of actin in solution with the desired GdmCl concentration.

To clarify the process of GdmCl-induced formation of inactivated actin kinetic curves reflecting the denaturant-induced changes in intensity of intrinsic fluorescence were recorded [95]. At low GdmCl concentrations (below 1.0 M) the fluorescence intensity decreases monotonously with time, slowly approaching its equilibrium values (Fig. 9). At high GdmCl concentrations (above 3.0 M) intensity of the actin intrinsic fluorescence also decreases monotonously, and rapidly approaches the value typical of the completely unfolded protein (Fig. 9). The most intriguing results were obtained for moderate GdmCl concentrations from 1.0 to 2.0 M. Within this concentration range, the fluorescence intensity first decreases over time, but then increases slowly to the equilibrium value (Fig. 9B).

The minimum seen in the kinetic curves at 1.0, 1.2, 1.5, and 1.8 M GdmCl suggests that the transition from the native to inactivated state occurs via some intermediate state in which the fluorescence intensity is lower than in the native and the inactivated states (Fig. 9A). Actin in completely unfolded state has been known to have the lowest intensity at 320 nm compared with native and inactivated actin (Fig. 2). Therefore it is suggested that inactivated actin is formed from native actin via essentially unfolded state.

The same shape of the kinetic curves was found for other spectroscopic characteristics, which values for unfolded actin were lower than that for native and inactivated states and which, unlike fluorescence intensity, define the structure of protein qualitatively. Kinetic curves measured at 1.0–2.0 M GdmCl for parameter *A* that reflects the fluorescence spectrum position and shape (Fig. 10) and fluorescence anisotropy (Fig. 11) also were characterized by specific minimum. The value of fluorescence anisotropy is known to decrease with increase of mobility of chromophore. Thus, association of protein

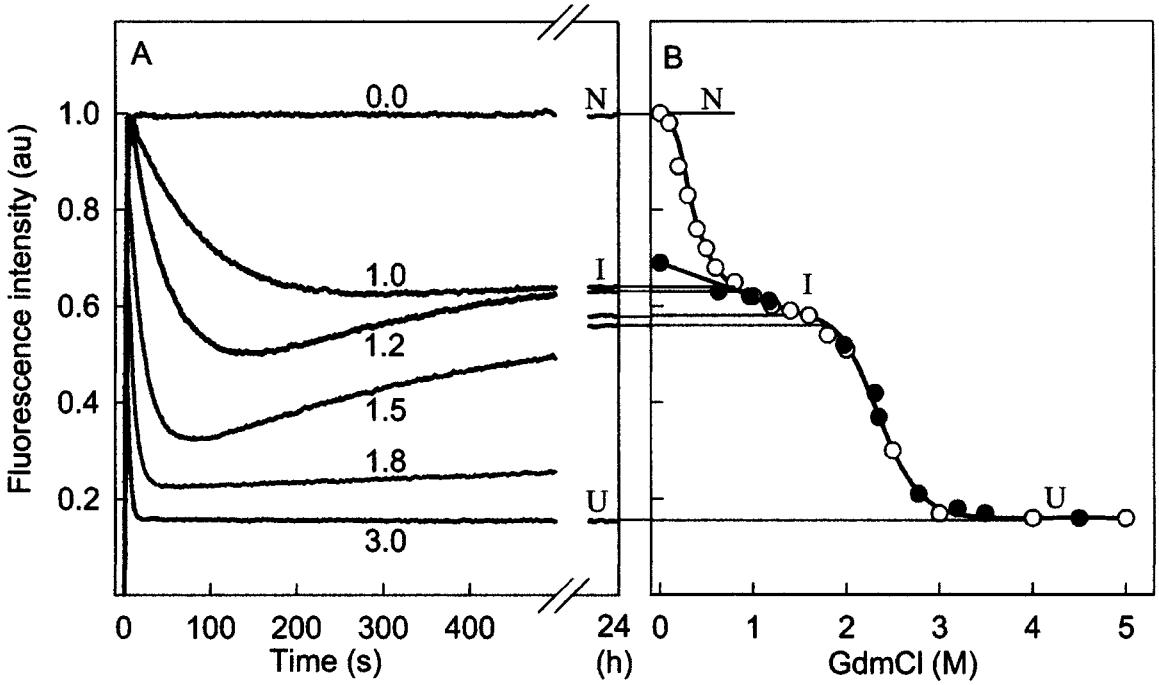

Fig. 9. Actin denaturation monitored by the change of intrinsic fluorescence intensity at 320 nm. A, Kinetics of actin denaturation induced by GdmCl. The values on the curves are the concentration of GdmCl. B. The fluorescence intensity of actin recorded after 24 h of incubation in the definite concentrations of GdmCl. Open and black symbols correspond to the unfolding and refolding experiments, respectively. In the experiment of refolding the appropriate concentration of GdmCl were obtained by dilution of actin solution in 5M GdmCl. Protein concentration was 0.1 mg/ml, λ_{ex} = 297 nm, λ_{em} = 320 nm.

molecules is usually accompanied by anisotropy increase, whereas dissociation of oligomers and unfolding of protein result in anisotropy decrease. In agreement with this,

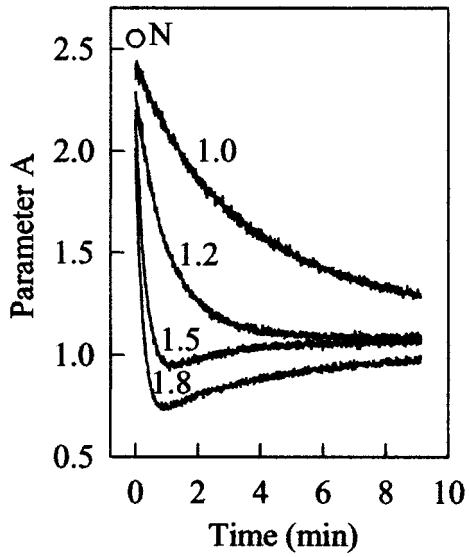

Fig. 10. Kinetics of actin denaturation monitored by the change of parameter $A = I_{320}/I_{365}$. The values on the curves are the final concentration of GdmCl. λ_{ex} = 297 nm.

Figure 11 shows that formation of inactivated actin (which was shown to be a 15-mer [63,64]) is accompanied by an essential increase of fluorescence anisotropy. On the other hand, the unfolding of protein is characterized by a pronounced drop of the anisotropy value. The combination of these two processes results in the appearance of minimum of the kinetic curve of fluorescence anisotropy at moderate GdmCl concentration (1.2 M). This means that actin essentially unfolds before the appearance of the inactivated conformation. Importantly, with time values of parameter *A* and fluorescence anisotropy were approaching the values typical of inactivated actin.

Based on all experimental data, the following scheme of actin unfolding was proposed

$$\mathrm{N} \xrightarrow{k_1} \mathrm{U}^* \underset{k_3}{\overset{k_2}{\rightleftarrows}} \mathrm{I} \qquad (9)$$

The calculation of the rate constants k_1, k_2, and k_3 performed in assumption that fluorescence intensity I_{320} for kinetic intermediate U* equals to that of completely unfolded state U, showed a good agreement between the calculated and experimental kinetic curves of fluorescence intensity (Fig. 12). To characterize the fluorescence

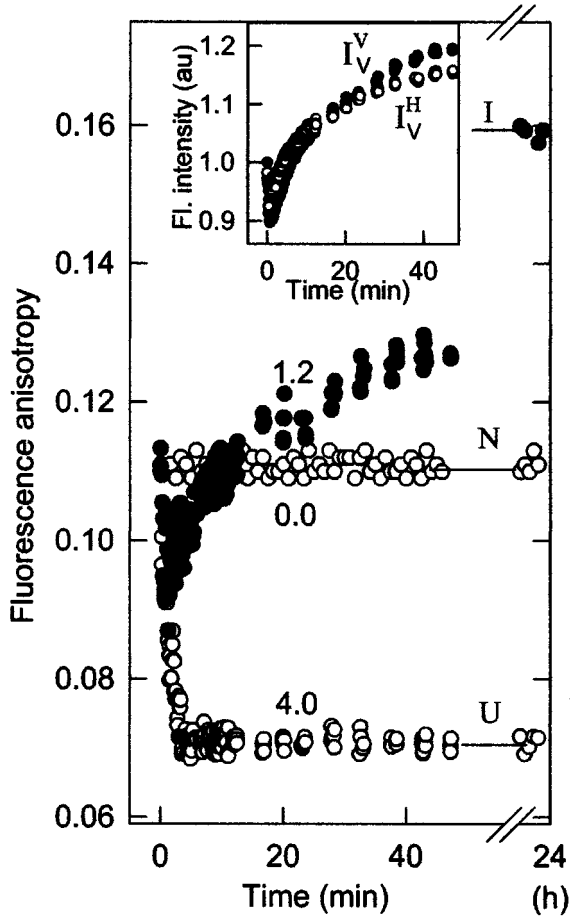

Fig. 11. Kinetics of actin denaturation monitored by the change of fluorescence anisotropy. The values on the curves are the concentration of GdmCl. λ_{ex} = 297 and λ_{em} = 365 nm.

properties of actin in the state U* wherever possible, and to elucidate whether the fluorescence spectra of actin in the states U and U* coincide or differ the parametric dependences of fluorescence intensity recorded at 320 and 365 nm were constructed (Fig. 13). Before analyzing the obtained dependences it is necessary to elucidate the main points of this approach.

Detection of Intermediate States and Study of Their Properties by Construction of the Parameter Dependences of Two Independent Extensive System Characteristics

Extensive characteristics are the characteristics whose value changes proportionally with the substance of the system under examination. Any extensive characteristic of the system consisting of two components is determined by

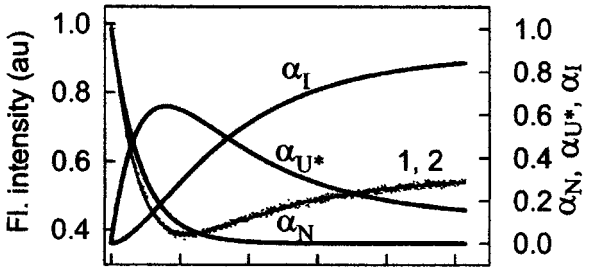

Fig. 12. The analysis of the kinetic curve of actin denaturation by 1.2 M GdmCl. Curve 1 (points), I_{exper}, the experimental fluorescence intensity. Curve 2, $I_{calc} = \alpha_N I_N + \alpha_U I_U + \alpha_I I_I$, the calculated best fit of the fluorescence intensity that corresponds to the values $k_1 = 2.1 \cdot 10^{-2}$, $k_2 = 7.2 \cdot 10^{-3}$, and $k_3 = 7.6 \cdot 10^{-4} s^{-1}$. Here I_N, I_U and I_I are fluorescence intensities and α_N, α_U and α_I are the fractions of actin molecule in native, unfolded and inactivated states, respectively, $\alpha_N + \alpha_U + \alpha_I = 1$. Time dependences of the values of α_N, α_U, and α_I are shown. The rate constants k_i were determined from the minimization of the sum of the squares residuals $\Phi = \sum_i (I_{exp\,er}(t) - I_{calc}(t))^2$, taking into account that for kinetic scheme (2) $\alpha_N = \exp(-k_1 t)$; $\alpha_U = (-k_2 k_1 \exp(-k_1 t) + k_3 k_2 \exp(-k_1 t) - k_3 k_1 \exp(-K_1 t) + k_3^2 \exp(-k_1 t) - k_3 k_2 + k_3 k_1 - k_3^2 + k_2 k_1 \exp(-(k_2 + k_3)t))/((k_2 + k_3)(k_1 - k_2 - k_3))$; $\alpha_1 = -k (k_1 \exp(-(k_2 + k_3) t) - k_2 \exp(-k_1 t) - k_3 \exp(-k_1 t) - k_1 + k_2 + k_3)/((k_2 + k_3)(k_1 - k_2 - k_3))$.

$$I(\theta) = \alpha_1(\theta) I_1 + \alpha_2(\theta) I_2 \qquad (10)$$

where I_1 and I_2 are the values of $I(\theta)$, at 100% content of the first and the second component, respectively, and $\alpha_1(\theta)$ и $\alpha_2(\theta)$ are the relative fraction of this components in the system, $\alpha_1(\theta) + \alpha_2(\theta) = 1$, θ is any parameter depending of which the content of the components is changed. Denaturant concentration, temperature, pH of the solution, etc. can be taken as a parameter. Only for extensive characteristics (as opposed to intensive characteristics such as fluorescence spectrum position, parameter *A*, fluorescence anisotrophy, etc.) which provide qualitative characterization of the system, Eq. (10) is valid and the fraction of the components in the system, as well as the equilibrium constant *K* can be determined by simple equations

$$\alpha_1(\theta) = \frac{I(\theta) - I_2}{I_1 - I_2}, \quad \alpha_2(\theta) = \frac{I_1 - I(\theta)}{I_1 - I_2},$$

$$K(\theta) = \frac{I_1 - I(\theta)}{I(\theta) - I_2} \qquad (11)$$

If intensive characteristics are used these equations for determination $\alpha_1(\theta)$, $\alpha_2(\theta)$, and $K(\theta)$ are not valid [4], although this often is not taken into account in studies of protein conformation transition.

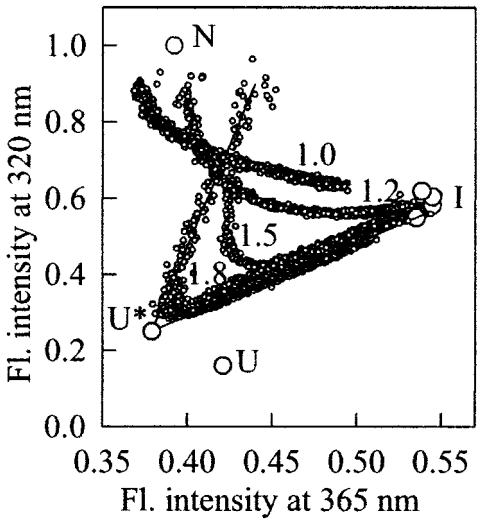

Fig. 13. Actin denaturatioin induced by GdmCl. Parametric dependences of fluorescence intensity at 320 and at 365 nm, parameter is the time from the beginning of denaturation. The values on the curves are the concentration of GdmCl. Fluorescence characteristics of native (N), essential unfolded intermediate (U*), inactivated (I) and completely unfolded (U) actin are indicated. Protein concentration was 0.44 mg/ml, λ_{ex} = 297 nm.

Fluorescence intensities at 320 and 365 nm can be taken as two independent extensive characteristics of the system. In this case

$$I_{320}(\theta) = \alpha_1(\theta)I_{1,320} + \alpha_2(\theta)I_{2,320} \qquad (12)$$

and

$$I_{365}(\theta) = \alpha_2(\theta)I_{1,365} + \alpha_2(\theta)I_{2,365}. \qquad (13)$$

Eliminating $\alpha_1(\theta)$ and $\alpha_2(\theta)$ from Eqs. (12) and (13), the dependence between $I_{320}(\theta)$ and $I_{365}(\theta)$ can be obtained

$$I_{320}(\theta) = a + bI_{365}(\theta) \qquad (14)$$

where

$$\alpha = I_{1,320} - \frac{I_{2,320} - I_{1,320}}{I_{2,365} - I_{1,365}}I_{1,365} \text{ and } b = \frac{I_{2,320} - I_{1,320}}{I_{2,365} - I_{1,365}}$$

Eq. (14) means that if with change of the parameter θ the transition between the states 1 and 2 follows the model "all or none" without the appearance of the intermediate states, the parametric dependence between any two extensive characteristics must be linear. If the experimentally recorded parametric dependence between two extensive characteristics of the system is not linear, it unequivocally means that the process of the transition from the initial to the final state is not one-stage process but it proceeds with formation of one or several intermediate states.

The approach to analyze proteins conformational transition based on the base of construction of parametric dependences of the fluorescence intensity recorded at two different wavelengths was proposed as early as in 1976 by Burshtein [46], but in subsequent years was used only a few times (see, e.g., [40]). We have used this approach to prove the multitude of the intermediate states which appear on denaturation of carbonic anhydrase II [96] and creatine kinase [97] by GdmCl. In the work on actin folding-unfolding [98] this approach has been used for the first time to analyze results of kinetic experiments.

Properties of the Kinetic Predecessor of Inactivated Actin

The parametric dependences of I_{320} on I_{365} were constructed based on the recorded kinetic process of actin unfolding induced by GdmCl. In these experiments the fluorescence intensities recorded at the wavelengths 320 and 365 nm were used as independent extensive characteristics and the time from the moment of the protein solution mixture with GdmCl was taken as a parameter. The results of previous study of the GdmCl-induced actin denaturation [95] indicate that the rate constant of the process N → U* (k_1) increases with the elevation of the GdmCl final concentration, while the rate constant of inactivated actin formation U* → I (k_2) decreases. The relation between k_1 and k_2 is such that the processes N → U* and U* → I are separated in time at 1.8 M GdmCl. Therefore, the corresponding parametric dependence of I_{320} on I_{365}, presented in Figure 13, can be approximated by two practically straight lines. It is evident that the cross point of these two lines characterizes the fluorescence properties of actin in the U* state. The mean values of the fluorescence intensities of actin in U* state are $(I_{U*}/I_N)_{320} = 0.25$ and $(I_{U*}/I_N)_{365} = 0.97$, whereas for actin in the completely unfolded state these values are 0.16 and 1.08 respectively. Many times repeated measurements of kinetic dependences allow concluding that $A_{U*} > A_U$, $I_{320,U*} > I_{320,U}$ and $I_{365,U*} < I_{365,U}$. The latter might be because the intrinsic tryptophan residues Trp340 and Trp356, which contribute significantly to the fluorescence spectrum of native actin [23] retain in this state slightly more blue fluorescence spectrum than that in the unfolded state U, while tryptophan residues Trp79 and Trp86, which fluorescence spectrum is red shifted, but the contribution to the fluorescence spectrum of native actin is small, in the U* state remain quenched by sulfur atoms of cysteine and methionine residues.

Thus, the obtained data allow concluding that fluorescence properties of the kinetic intermediate U* differs from that of actin in 4–6 M GdmCl. The kinetic interme-

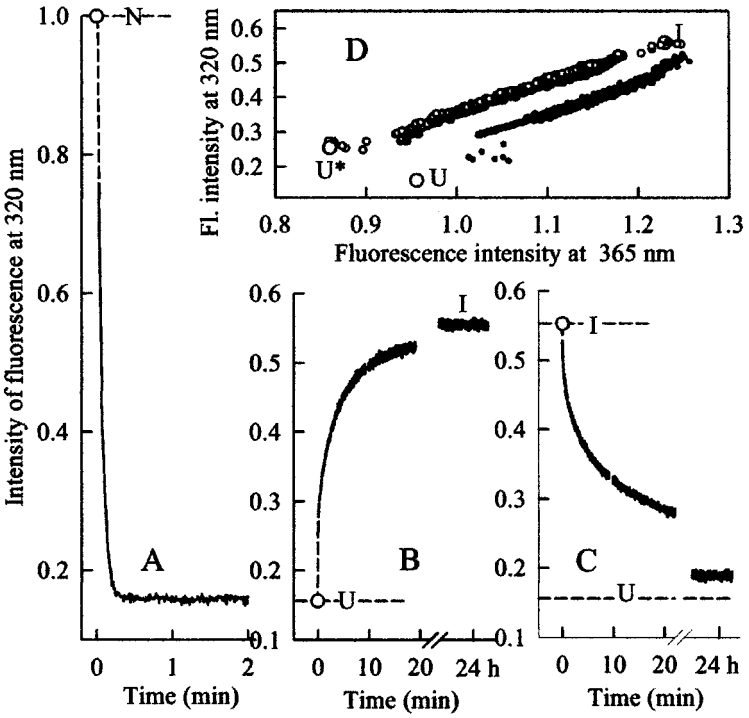

Fig. 14. Inactivated actin denaturation-renaturation induced by the change of GdmCl content in solution. Kinetics of the change of intrinsic fluorescence intensity at 320 nm. A, Denaturation of native actin induced by 4.0 M GdmCl. B, Actin renaturation from 4,0 M GdmCl (final concentration of GdmCl was 1.8 M). C, Denaturation of inactivated actin induced by 4.0 M GdmCl. D, Parametric dependences of fluorescence intensity at 320 and at 365 nm, parameter is the time from the beginning of denaturation (curve 1) or renaturation (curve 2).

diate has more blue fluorescence spectrum in comparison with completely unfolded state of actin. It has been shown that in the U* state elements of secondary structure are retained. At the same time, ANS does not bind to actin in this state. In total these data substantiate suggestion that the U* state is premolten globule. With decrease of GdmCl concentration the parametric dependences of I_{320} on I_{365} progressively differ from that obtained for 1.8 M GdmCl (Fig. 13). Nonetheless, their character indicates that the process of inactivation of actin formation proceeds via the state of essential protein unfolding, although the lifetime of this state decreases with the reduction of the final concentration of GdmCl. Unexpectedly, it was found that the parametric dependences of I_{320} on I_{365} originated not from the single point corresponding to the native state of actin in the absence of GdmCl, but from different points (Fig. 13). It means that the change of the solution leads to a rapid change of fluorescence properties of actin. At present it is not clear weather the recorded effects are determined by structural changes of protein or simply by the change of the solution content, that affects the fluorescence properties of Trp79, partially exposed to the solvent although its contribution to the bulk fluorescence of actin is not large.

Kinetics of the Transition Inactivated Actin-Completely Unfolded State

The examination of the folding-unfolding process of actin and the place of inactivated actin and its kinetic predecessor in these processes would be incomplete without considering transition between the inactivated and completely unfolded state. The results of steady-state investigation [45,63,95] indicate that this process is reversible and occurs in the range of GdmCl concentration from 1.8 to 3.5 M with the middle point at 2.5 M (Fig. 7). The kinetic measurements of the changes of fluorescence intensity in the course of the protein transition from 1.8 M to 4.0 M GdmCl and vice versa performed in the present work proved the general conclusion made earlier (Figs. 14B and 14C). But it was found that the U $\rightarrow$ I transition is faster than the inverse process I $\rightarrow$ U. The unfolding of inactivated actin is incomplete even within 24 h after its transform to 4 M GdmCl (Fig. 14C). Interest-

ingly, the complete unfolding of native actin after its transform to 4 M GdmCl is completed within the first 10 s. Both I → U and U → I processes seem to be not one-step processes as indicated by the character of parametric dependences of I_{320} on I_{365} of these processes (Fig. 14D) and impossibility to represent them by monoexponential law to which the kinetics of one-step processes follows. It seems likely that the transition from the completely unfolded state to the inactivated state passes through the kinetic intermediate U* (Fig. 14D, curve 1). When the solutions are mixed manually this U → U* process occurs within the dead time of experiment.

New Kinetic Scheme of Actin Folding-Unfolding

All the obtained data in total allowed to propose the kinetic scheme of the actin protein-unfolding induced by GdmCl [98]

$$\mathrm{N} \rightarrow \mathrm{N}^* \rightarrow \begin{array}{c} \mathrm{U}^* \\ \Uparrow\Downarrow \\ \mathrm{I} \end{array} \rightleftarrows \mathrm{U} \qquad (15)$$

In this kinetic scheme it is not completely understood the nature of the state N* which precedes the transformation of native actin into the essentially unfolded state U* and which fluorescent properties depend on GdmCl concentration. Meanwhile the appearance of the essentially unfolded state U* which precedes the appearance of completely unfolded state or misfolded state which structure is stabilized by aggregation of partially-folded macromolecules of the protein, known as inactivated actin I, may be considered to be proved. These results also may be essential for the search for pathways of actin folding in vitro.

ACKNOWLEDGMENTS

This work was supported by Russian Foundation of Basic Research (Grants 00-04-49224, 01-04-49308, 02-04-81013, 03-04-49387) and INTAS (Grant 2001-2347). We are very grateful to Dr. A. M. Surin for valuable discussions.

REFERENCES

1. J. R. Lakowicz (1999) Principles of Fluorescence Spectroscopy, 2nd Ed. Kluwer Academic/Plenum Publishers, New York.
2. M. R. Eftink (1991) Fluorescence techniques for studying protein structure. *Methods Biochem Anal.* **35**, 127–205.
3. A. P. Demchenko (1986) Fluorescence analysis of protein dynamics. *Essay Biochem.* **22**, 120–157.
4. M. R. Eftink (1998) The use of fluorescence methods to monitor unfolding transitions in proteins. *Biokhimiya* (Moscow) **63**, 327–337.
5. E. A. Burshtein (1976) Intrinsic Protein Fluorescence: Origin and Applications. *Ser. Biophysics, vol. 7*, VINIITI, Moscow.
6. Y. Chen and M. D. Barkley (1998) Toward understanding tryptophan fluorescence in proteins. *Biochemistry* **37**, 9976–9982.
7. Y. Chen, B. Liu, H.-T. Yu, and M. D. Barkley (1996) The peptide bond quenches indole fluorescence. *J. Am. Chem. Soc.* **118**, 9271–9278.
8. H.-T. Yu, M. A. Vela, F. R. Fronczek, M. L. McLaughlin, and M. D. Barkley (1995) Microenvironmental effects on the solvent quenching rate in constrained tryptophan derivatives. *J. Am. Chem. Soc.* **117**, 348–357.
9. L. Tilstra, M. C. Sattler, W. R. Cherry, and M. D. Barkley (1990) Fluorescence of a rotationally constrained tryptophan derivative, 3-carboxy-1,2,3,4-tetrahydro-2-carboline. *J. Am. Chem. Soc.* **112**, 9176–9182.
10. W. J. Colucci, L. Tilstra, M. C. Sattler, F. R. Fronczek, and M. D. Barkley (1990) Conformational studies of a constrained tryptophan derivative: implications for the fluorescence quenching mechanism. *J. Am. Chem. Soc.* **112**, 9182–9190.
11. L. P. McMahon, H.-T. Yu, M. A. Vela, G. A. Morales, L. Shui, F. R. Fronczek, M. L. McLaughlin, and M. D. Barkley (1997) Conformation interconversion in the excited state of constrained tryptophan derivatives. *J. Phys. Chem.* **B 101**, 3269–3280.
12. J. R. Lakowicz (2000) On spectral relaxation in proteins. *Photochem. Photobiol.* **72**, 421–437.
13. P. R. Callis (1997) ^1L_a and ^1L_b transitions of tryptophan: applications of theory and experimental observations to fluorescence of proteins. *Methods Enzymol.* **278**, 113–150.
14. J. T. Vivian and P. R. Callis (2001) Mechanisms of tryptophan fluorescence shifts in proteins. *Biophys. J.* **80**, 2093–2109.
15. E. A. Burstein, S. M. Abornev, and Y. K. Reshetnyak (2001) Decomposition of protein tryptophan fluorescence spectra into log-normal components. I. Decomposition algorithms. *Biophys. J.* **81**, 1699–1709.
16. Y. K. Reshetnyak and E. A. Burstein (2001) Decomposition of protein tryptophan fluorescence spectra into log-normal components. II. The statistical proof of discreteness of tryptophan classes in proteins. *Biophys. J.* **81**, 1710–1734.
17. Y. K. Reshetnyak, Y. Koshevnik, and E. A. Burstein (2001) Decomposition of protein tryptophan fluorescence spectra into log-normal components. III. Correlation between fluorescence and microenvironment parameters of individual tryptophan residues. *Biophys. J.* **81**, 1735–1758.
18. K. K. Turoverov, I. M. Kuznetsova, and V. N. Zaitzev (1985) The environment of the tryptophan residue in pseudomonas aeruginosa azurin and its fluorecsence properties. *Biophys. Chem.* **23**, 79–89.
19. F. C. Bernstein, T. F. Koetzle, G. J. B. Williams, E. F. Meyer Jr., M. D. Brice, J. R. Rodgers, O. Kennard, T. Shimanouchi, and M. Tasumi (1977) The Protein Data Bank: a computer-based archival file for macromolecular structures. *J. Mol. Biol.* **112**, 535–542.
20. K. K. Turoverov and I. M. Kuznetsova (1986) What causes the depolarization of trypsin and trypsinogen fluorescence. Intramolecular mobility or non-radiative energy transfer? *Biophys. Chem.* **25**, 315–323.
21. T. V. Agekyan, S. I. Bezborodova, I. M. Kuznetsova, K. M. Polyakov, and K. K. Turoverov (1988) Spectral and polarizational characteristics of ribonuclease C_2. Unusual fluorescence of tyrosine residues. *Mol. Biol.* **22**, 612–623.
22. I. M. Kuznetsova, O. A. Antropova, K. K. Turoverov, and S. Yu. Khaitlina (1996) Conformational changes in subdomain I of actin induced by proteolytic cleavage within the DNase I-binding loop: energy transfer from tryptophan to AEDANS. *FEBS Lett.* **383**, 105–108.
23. I. M. Kuznetsova, T. A. Yakusheva, and K. K. Turoverov (1999) Contribution of separate tryptophan residues to intrinsic fluorescence of actin. Analysis of 3D structure. *FEBS Lett.* **452**, 205–210.

24. I. M. Kuznetsova, A. G. Biktashev, L. N. Malova, N. A. Bushmarina, V. N. Uversky, and K. K. Turoverov (2000) Understanding the contribution of individual tryptophan residues to intrinsic lysozyme fluorescence. *Protein Peptide Lett.* **7**, 411–420.
25. L. G. Martensson, P. Jonasson, P. O. Freskgard, M. Svensson, U. Carlsson, and B. H. Jonsson (1995) Contribution of individual tryptophan residues to the fluorescence spectrum of native and denatured forms of human carbonic anhydrase II. *Biochemistry* **34**, 1011–1021.
26. V. Gopalan, R. Golbik, G. Schreiber, A. R. Fersht, and S. Altman (1997) Fluorescence properties of a tryptophan residue in an aromatic core of the protein subunit of ribonuclease P from Escherichia coli. *J. Mol. Biol.* **267**, 765–769.
27. W. M. Atkins, P. S. Stayton, and J. J. Villafranca (1991) Time-resolved fluorescence studies of genetically engineered Escherichia coli glutamine synthetase. Effects of ATP on the tryptophan-57 loop. *Biochemistry* **30**, 3406–3416.
28. T. C. Doyle, J. E. Hansen, and E. Reisler (2001) Tryptophan fluorescence of yeast actin resolved via conserved mutations. *Biophys. J.* **80**, 427–434.
29. P. Sheterline, J. Clayton, and J. Sparrow (1998) *Actin. Protein Profile*. Oxford University Press, Oxford.
30. T. D. Pollard, L. Blanchoin, and R. D. Mullins (2000) Molecular mechanism controlling actin filament dynamics in nonmuscle cells. *Annu. Rev. Biophys. Biomol. Struct.* **29**, 545–576.
31. W. Kabsch, H. G. Mannherz, D. Suck, E. F. Pai, and K. C. Holmes (1990) Atomic structure of the actin: DNase I complex. *Nature* **347**, 37–44.
32. P. J. McLaughlin, J. T. Gooch, H. G. Mannherz, and A. G. Weeds (1993) Structure of gelsolin segment 1-actin complex and the mechanism of filament severing. *Nature* **364**, 685–692.
33. R. C. Robinson, M. Mejillano, V. P. Le, L. D. Burtnick, H. L. Yin, S. Choe (1999) Domain movement in gelsolin: a calcium-activated switch. *Science* **286**, 1939–1942.
34. C. E. Schutt, J. C. Myslik, M. D. Rozycki, N. C. Goonesekere, and U. Linberg (1993) The structure of crystalline profiling-β-actin. *Nature* **365**, 810–816.
35. L. R. Otterbein, P. Graceffa, and R. Dominquez (2001) The crystal structure of uncomplexed actin in the ADP state. *Science* **293**, 708–711.
36. K. K. Turoverov, S. Yu. Khaitlina, and G. P. Pinaev (1976) Ultraviolet fluorescence of actin. Determination of native actin content in actin preparations. *FEBS Lett.* **62**, 4–7.
37. S. S. Lehrer and G. Kerwar (1972) Intrinsic fluorescence of actin. *Biochemistry* **11**, 1211–1217.
38. A. Finazzi-Agro, G. Rotilio, L. Avigliano, P. Guerrieri, V. Boffi, and B. Mondovi (1970) Environment of copper in Pseudomonas fluorescens azurin: fluorometric approach. *Biochemistry* **9**, 2009–2014.
39. Yu. Yamamoto and J. Tanaka (1970) Spectroscopic studies on the configurational structures of ribonuclease T1. *Biochim. Biophys. Acta* **207**, 522–531.
40. E. A. Permyakov, V. V. Yarmolenko, V. I. Emelyanenko, E. A. Burstein, J. Closset, and C. Gerday (1980) Fluorescence studies of the calcium binding to whiting (Gadus merlangus) parvalbumin. *Eur. J. Biochem.* **109**, 307–315.
41. I. M. Kuznetsova and K. K. Turoverov (1998) What determines the characteristics of protein intrinsic fluorescence? Analysis of tryptophan residue localization in proteins. *Tsitologia* **40**, 747–762.
42. S. H. Gellman and D. N. Woolfson (2002) Mini-proteins Trp the light fantastic. *Nature Struct. Biol.* **9**, 408–410.
43. J. W. Neidigh, R. M. Fesinmeyer, and N. H. Andersen (2002) Designing a 20-residue protein *Nature Struct. Biol.* **9**, 425–430.
44. M. Eftink and C. A. Ghiron (1981) Fluorescence quenching studies with proteins. *Anal. Biochem.* **114**, 199–227.
45. K. K. Turoverov, A. G. Bictashev, S. Yu. Khaitlina, and I. M. Kuznetsova (1999) The structure and dynamics of partially-folded actin. *Biochemistry* **38**, 6261–6269.
46. E. A. Burstein (1976) Luminescence of protein chromophors (model investigations). *Ser. Biophysica, vol. 6*, VINITI, Moscow.
47. Th. Forster (1960) Transfer mechanisms of electronic excitation energy. *Rad. Res. Suppl.* **2**, 326–339.
48. R. E. Dale and J. Eisinger (1974) Intramolecular distances determined by energy transfer. Dependence on orientational freedom of donor and acceptor. *Biopolymers* **13**, 1573–1605.
49. J. Eisinger, B. Feuer, and A. A. Lamola (1969) Intramolecular singlet excitation transfer. Applications to polypeptides. *Biochemistry* **8**, 3908–3915.
50. I. Z. Steinberg (1971) Long-range nonradiative transfer of electronic excitation energy in proteins and polypeptides. *Ann. Rev. Biochem.* **40**, 83–114.
51. I. M. Kuznetsova, S. Yu. Khaitlina, and K. K. Turoverov (1998) Structural properties of inactivated actin: an intermediate form in the folding-unfolding of actin. *Bioorganic Chem. (Moscow)* **24**, 783–791.
52. H. Strzelecka-Golaszewska, S. Yu. Venyaminov, S. Zmorzynski, and M. Mossakowska (1985) Effect of various amino acid replacements on the conformational stability of G-actin. *Eur. J. Biochem.* **147**, 331–342.
53. B. Nagy and W. P. Jencks (1962) Optical rotatory dispersion of G-actin. *Biochemistry* **1**, 987–996.
54. J. J. West, B. Nagy, and J. Gergely (1967) Free adenosine diphosphate as an intermediary in the phosphorylation by creatine phosphate of adenosine diphosphate bound to actin. *J. Biol. Chem.* **242**, 1140–1145.
55. B. Nagy and H. Strzelecka-Golaszewska (1972) Optical rotatory dispersion and circular dichroic spectra of G-actin. *Arch. Biochem. Biophys.* **150**, 428–435.
56. H. Strzelecka-Golaszewska, B. Nagy, and J. Gergely (1974) Changes in conformation and nucleotide binding of Ca, Mn or MgG-actin upon removal of the bound divalent ion. Studies of ultraviolet difference spectra and optical rotation. *Arch. Biochem. Biophys.* **161**, 559–569.
57. C. C. Contaxis, C. C. Bigelow, and C. G. Zarkadas (1977) The thermal denaturation of bovine cardiac G-actin. *Can. J. Biochem.* **55**, 325–331.
58. L. V. Tatunashvili and P. L. Privalov (1984) Calorimetric study of G-actin denaturation *Biofizika (Moscow)* **29**, 583–585.
59. I. M. Kuznetsova, S. Yu. Khaitlina, S. N. Konditerov, A. M. Surin, and K. K. Turoverov (1988) Changes of structure and intramolecular mobility in the course of actin denaturation. *Biophys. Chem.* **32**, 73–78.
60. A. Bertazzon, G. H. Tian, A. Lamblin, and T. Y. Tsong (1990) Enthalpic and entropic contributions to actin stability: Calorimetry, circular dichroism and fluorescence study and effect of calcium. *Biochemistry* **29**, 291–298.
61. T. Le Bihan and C. Gicquaud (1993) Kinetic study of the thermal denaturation of G actin using differential scanning calorimetry and intrinsic fluorescence spectroscopy. *Biochem. Biophys. Res. Comm.* **194**, 1065–1073.
62. H. Schuler, U. Lindberg, C. E. Schutt, and R. Karlsson (2000) Thermal unfolding of G-actin monitored with the DNase I-inhibition assay stabilities of actin isoforms. *Eur. J. Biochem.* **267**, 476–486.
63. I. M. Kuznetsova, A. G. Biktashev, S. Yu. Khaitlina, K. S. Vassilenko, K. K. Turoverov, and V. N. Uversky (1999) Effect of self-association on the structural organization of partially folded proteins: inactivated actin. *Biophys. J.* **77**, 2788–2800.
64. I. M. Kuznetsova, K. K. Turoverov, and V. N. Uversky, (1999) Unusual combination of the distorted structure and frozen internal mobility in inactivated actin molecule. *Protein Peptide Lett.* **6**, 73–78.
65. A. G. Szabo and D. M. Rayner (1980) Fluorescence decay of trytophan conformers in aqueous solution. *J. Am. Chem. Soc.* **102**, 554–563.

66. I. M. Kuznetsova and K. K. Turoverov (1983) Polarization of intrinsic fluorescence of proteins. III. Intramolecular mobility of trytophan residues. *Mol. Biol. (Moscow)* **17**, 741–754.
67. K. K. Turoverov and I. M. Kuznetsova (1998) What determines the characteristics of protein intrinsic fluorescence? Analysis of tryptophan residue localization in proteins. *Tsitologiia (St. Petersburg)* **40**, 735–746.
68. I. M. Kuznetsova, K. K. Turoverov, and V. N. Uversky (1999) Inactivated actin, and aggregate comprised of partially-folded monomers, has a overall native-like packing density. *Protein Peptide Lett.* **6**, 173–178.
69. L. R. De Young, A. L. Fink, and K. Dill (1993) Aggregation of globular proteins. *Acc. Chem. Res.* **26**, 614–620.
70. L. R. De Young, K. Dill, and A. L. Fink (1993) Aggregation and denaturation of apomyoglobin in aqueous urea solutions. *Biochemistry* **32**, 3877–3886.
71. K. Oberg, B. A. Chrunyk, R. Wetzel, and A. L. Fink (1994) Native-like secondary structure in interleukin-1/b inclusion bodies by attenuated total reflectance FTIR. *Biochemistry* **33**, 2628–2634.
72. A. L. Fink (1995) Molten globules. *Methods Mol. Biol.* **40**, 343–360.
73. A. L. Fink (1995) Compact intermediate states in protein folding. *Ann. Rev. Biophys. Biomol. Struct.* **24**, 495–522
74. G. V. Semisotnov, H. Kihara, N. V. Kotova, K. Kimura, Y. Amemiya, K. Wakabayashi, I. N. Serdyuk, A. A. Timchenko, K. Chiba, K. Nikaido, T. Ikura, and K. Kuwajima (1996) Protein globularization during folding. A study by synchrotron small-angle X-ray scattering. *J. Mol. Biol.* **262**, 559–574.
75. J. W. Kelly (2000) Mechanisms of amyloidogenesis. *Nature Struct. Biol.* **7**, 824–826.
76. A. L. Fink (1998) Protein aggregation: folding aggregates, inclusion bodies and amyloid. *Fold. Des.* **3**, R9–23.
77. V. N. Uversky, D. J. Segel, S. Doniach, and A. L. Fink (1998) Association-induced folding of globular proteins. *Proc. Natl. Acad. Sci. U.S.A.* **95**, 5480–5483.
78. F. A. Marston (1986) The purification of eukaryotic polypeptides synthesized in Escherichia coli. *Biochem. J.* **240**, 1–12.
79. C. H. Schein (1990) Solubility as a function of protein structure and solvent components. *Biotechnology* **8**, 308–317.
80. S. Frankel, J. Condeelis, and L. Leinwand (1990) Expression of actin in Escherichia coli. Aggregation, solubilization, and functional analysis. *J. Biol. Chem.* **265**, 17980–17987.
81. R. Wetzel (1992) In A. R. Rees, A. R. Sternberg, and R. Wetzel (Eds.) Protein Engineering. A Practical Approach, IRL Press, Oxford, pp. 191–219.
82. R. Wetzel (1992) in T. J. Ahern and M. C. Manning (Eds.) Stability of Protein Pharmaceuticals. Part B; In Vivo Pathways of Degradation and Strategies for Protein Stabilization, Plenum Press, New York. Vol. 3. pp. 43–88.
83. R. Wetzel (1994) Mutations and off-pathway aggregation of proteins. *Trends Biotechnol.* **12**, 193–198.
84. M. A. Speed, D. I. Wang, and J. King (1996) Specific aggregation of partially folded polypeptide chains: the molecular basis of inclusion body composition. *Nat. Biotechnol.* **14**, 1283–1287.
85. S. Massry and R. Glassock (1983) Textbook of Nephrology. Williams and Wilkins. Baltimore.
86. R. W. Carrell and B. Gooptu (1998) Conformational changes and disease-serpins, prions and Alzheimer's. *Curr. Opin. Struct. Biol.* **8**, 799–809.
87. J. Clark and J. Steele (1992) Phase-separation inhibitors and prevention of selerate cataract. *Proc. Natl. Acad. Sci. USA* **89**, 1720–1724.
88. J. W. Kelly (1997) Amyloid fibril formation and protein misassembly a structural quest for insights into amyloid and prion diseases. *Structure* **5**, 595–600.
89. J. D. Harper, P. T. Lansbury, Jr. (1997) Models of amyloid seeding in Alzheimer's disease and scrapie: mechanistic truths and physiological consequences of the time-dependent solubility of amyloid proteins. *Ann. Rev. Biochem.* **66**, 385–407.
90. E. H. Koo, P. T. Lansbury, Jr., J. W. Kelly (1999) Amyloid disease abnormal protein aggregation in neurodegeneration. *Proc. Natl. Acad. Sci. U.S.A.* **96**, 9989–9990.
91. J. W. Kelly (2002) Towards an understanding of amyloidogenesis. *Nat. Struct. Biol.* **9**, 323–325.
92. M. Hashimoto, and E. Masliah (1999) Alpha-synuclein in Lewy body disease and Alzheimer's disease. *Brain Pathol.* **9**, 707–720.
93. V. N. Uversky, A. Talapatra, J. R. Gillespie, and A. L. Fink (1999a) Protein deposits as the molecular basis of amyloidosis. Part I. Systemic amyloidoses. *Med. Sci. Monitor* **5**, 1001–1012.
94. V. N. Uversky, A. Talapatra, J. R. Gillespie, and A. L. Fink (1999b) Protein deposits as the molecular basis of amyloidosis. Part II. Localized amyloidosis and neurodegenerative disorders. *Med. Sci. Monitor* **5**, 1238–1254.
95. K. K. Turoverov, V. V. Verkhusha, M. M. Shavlovsky, A. G. Biktashev, O. I. Povarova, and I. M. Kuznetsova (2002) Kinetics of actin unfolding induced by guanidine hydrochloride. *Biochemistry* **41**, 1014–1019.
96. N. A. Bushmarina, I. M. Kuznetsova, A. G. Biktashev, K. K. Turoverov, and V. N. Uversky (2001) Partially folded conformations in the folding pathway of bovine carbonic anhydrase II: a fluorescence spectroscopic analysis. *ChemBioChem* **2**, 813–821.
97. I. M. Kuznetsova, O. V. Stepanenko, K. K. Turoverov, L. Zhu, J.-M. Zhou, A. L. Fink, and V. N. Uversky (2002) Unraveling multistate unfolding of rabbit muscle creatine kinase. *Biochim. Biophys. Acta* **1596**, 138–155.
98. I. M. Kuznetsova, V. V. Verkhusha, M. M. Shavlovsky, A. G. Biktashev, O. I. Povarova, O. V. Stepanenko, O. V. Stepanenko, and K. K. Turoverov (2002) The place of inactivated actin and its kinetic predecessor in actin folding-unfolding. *Biochemistry* **41**, 13127–13132.